EGU06-A-08334

Kinematic versus highly reduced-dynamic LEO orbits for global gravity field recovery

A. Jäggi, G. Beutler,
U. Hugentobler

EGU General Assembly, Vienna,
April 2-7, 2006

Introduction

We compare different high-low GPS-SST precise orbit determination (POD) methods for Low Earth orbiters (LEOs) in a simulation study to assess their capability to provide LEO positions suitable for a subsequent gravity field recovery (GFR).

Method 1 is an undifferenced GPS phase kinematic POD method [Svehla, 2004]. The LEO positions are derived independently from a priori gravity field information, but they are affected by rather large noise.

Method 2 is an undifferenced GPS phase reduced-dynamic POD method [Jäggi, 2005]. The LEO positions are less affected by noise, but they depend to some extent on a priori gravity field information.

We show where the trade-off between a desirable noise reduction and inacceptable a priori field dependencies can be found for method 2 for the purpose of GFR, and compare the results with those obtained from method 1.

Simulation of CHAMP GPS data:

EIGEN-2 [Reigber, 2003] up to deg. 90 served as the true geopotential model to generate a true CHAMP orbit over 4 days with all non-gravitational forces set to zero. High-low GPS-SST data with 10s or 30s sampling were then generated based on the true CHAMP orbit and the GPS final orbits.

CHAMP POD with the simulated GPS data:

Synthetic CHAMP positions were computed for the different scenarios defined by Tables 1 and 2. EIGEN-2 truncated at deg. 20 and with slightly erroneous coefficients up to deg. 20 (according to RMS errors provided with the EIGEN-2 model) served as the a priori model for Method 2, which is indicated by a vertical line in the corresponding figures to show the transition.

GFR with the synthetic CHAMP positions:

The synthetic CHAMP positions were used as uncorrelated pseudo-observations for GFR performed in the course of orbit determination (24h arcs, 6 Keplerian elements as arc-specific parameters).

30s vs. 10s GPS data

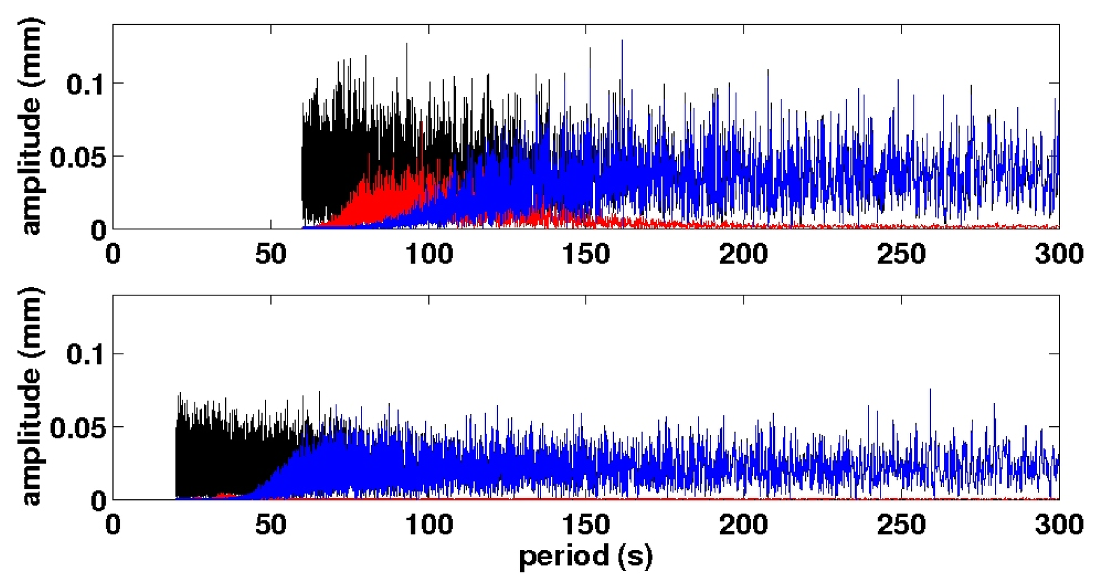

Figure 1: Spectra of orbit differences due to **Err.N** and **Err.A** (see Tables 1 and 2) for the solutions **2a** and due to **Err.N** for the solutions **1** over 4 days w.r.t. the true orbit for 30s (top) and 10s (bottom) sampling. Only the bottom solution of type **2a** is a possible candidate for GFR as **Err.A** has virtually no impact on the solution. Note the reduced high-frequency position noise for the solutions **2a** w.r.t. the solutions **1**.

AIUB
Poster compiled by Adrian Jäggi, March 2006
Astronomical Institute of the University of Bern
adrian.jaeggi@aiub.unibe.ch

Recovery based on 30s GPS data

	Method 1	Method 2		
Solution	**1**	**2a**	**2b**	**2c**
POD method	30s kin. coord.	60s r.d. acceler.	60s r.d. pulses	120s r.d. acceler.
Position sampling	30s	30s	30s	30s

Table 1: Simulated GPS phase zero-difference observations were used with 30s spacing to compute synthetic CHAMP orbits for 4 days with different POD methods. The computations were performed either in the sole presence of a 1mm white noise GPS phase RMS error (**Err.N**), or in the sole presence of the (systematic) a priori gravity field errors (**Err.A**), or in the presence of both error sources (**Err.N+A**).
In method 1 we solved for kinematic coordinates every 30s, which are not affected by **Err.A**. In method 2 we solved for pseudo-stochastic parameters with different time resolutions (solutions **2a**, **2b**, and **2c**) in a reduced-dynamic orbit determination procedure, which reduces **Err.N** in the orbit positions, but depends to some extent on **Err.A**. Note that orbits from method 2 would be identical to orbits from method 1 if pseudo-stochastic parameters were set up every 30s [Jäggi, 2005].
We used the 30s synthetic CHAMP orbit positions from solutions **1**, **2a**, **2b**, and **2c** for all 4 days for GFR. Fig. 2 displays the various solutions with different colors (indicating the method from Table 1) and line-styles (indicating the applied errors).

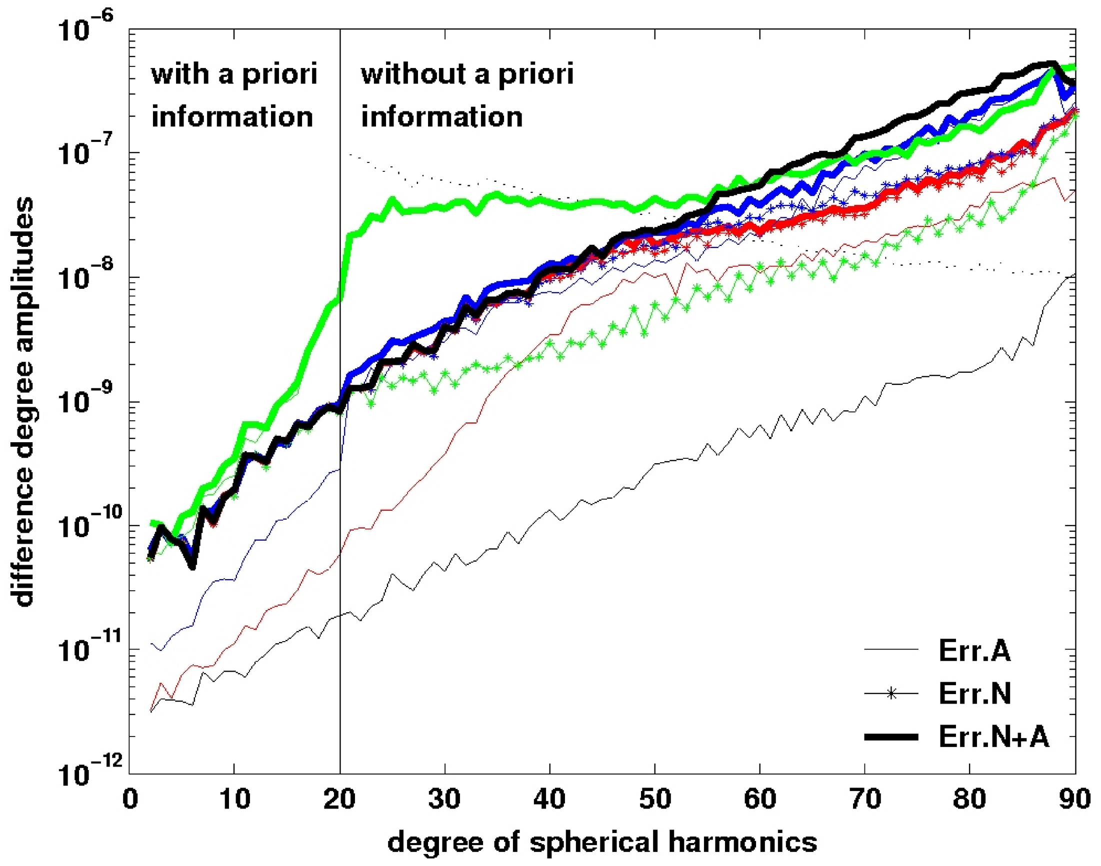

Figure 2: Deviations per degree of the estimated (fully normalized) spherical harmonics w.r.t. the true gravity field coefficients for the solutions **1**, **2a**, **2b**, and **2c**. Observe the varying contributions of **Err.N** and **Err.A** to the total effect **Err.N+A** for the different solutions. Deviations above the dashed line (= a priori model for deg.>20, i.e., zero model) indicate no signal content in the corresponding estimates.

Solution **1** is uniquely governed by **Err.N**, which limits the achievable resolution to deg. 53 in this simulation if only 4 daily batches are accumulated.

Solution **2a** performs slightly better than solution **1** for higher degrees due to the reduced high-frequency position noise (see Fig. 1 (top)). The solution is still dominated by **Err.N**, but a significant contribution due to **Err.A** can be observed already. As a matter of fact, **Err.A** would become dominant if more than about 20 daily batches had been accumulated.

Solution **2b** is partially dominated by **Err.A** as pulses compensate significantly worse for force model deficiencies than accelerations [Jäggi, 2006]. The solution performs worse than the solution **2a**.

Solution **2c** is completely dominated by **Err.A** and thus not useful for GFR, even if **Err.N** is greatly decreased due to the longer acceleration intervals.

Conclusion: The solutions **2a**, **2b**, and **2c** based on 30s GPS sampling are not well suited to derive unbiased gravity field information. A resolution of pseudo-stochastic parameters of at least 30s is required, which makes it necessary to process the full-rate GPS data.

Recovery based on 10s GPS data

	Method 1	Method 2	
Solution	**1**	**2a**	**2b**
POD method	10s kin. coord.	30s r.d. acceler.	30s r.d. pulses
Position sampling	10s / 30s / m	10s / 30s / m	30s

Table 2: Simulated GPS phase zero-difference observations were used with 10s spacing to compute synthetic CHAMP orbits for 4 days with different POD methods. The computations were performed either in the sole presence of **Err.N**, or in the sole presence of **Err.A**, or in the presence of **Err.N+A**. Note that orbits from method 2 are now (slightly) affected by **Err.A** despite the 30s parameter spacing.
We used the synthetic CHAMP orbit positions from solutions **1**, **2a**, and **2b** for all 4 days primarily with a 30s sampling (identically displayed in Fig. 3 as in Fig. 2) as pseudo-observations for GFR. Alternatively, we used the full, i.e., time consuming, 10s position sampling (marked by -x- in Fig. 3, x in solution color), or incorporated the 10s pseudo-observation equations into "mean" pseudo-observation equations which are set up every 30s (marked by -+- in Fig. 3, + in solution color).
For the sake of a better visibility, Fig. 3 displays the various solutions in the presence of **Err.A** and **Err.N+A** only. For the same reason, the alternative solutions marked by -x- and -+- are equally plotted with thin lines for **Err.A** and **Err.N+A**.

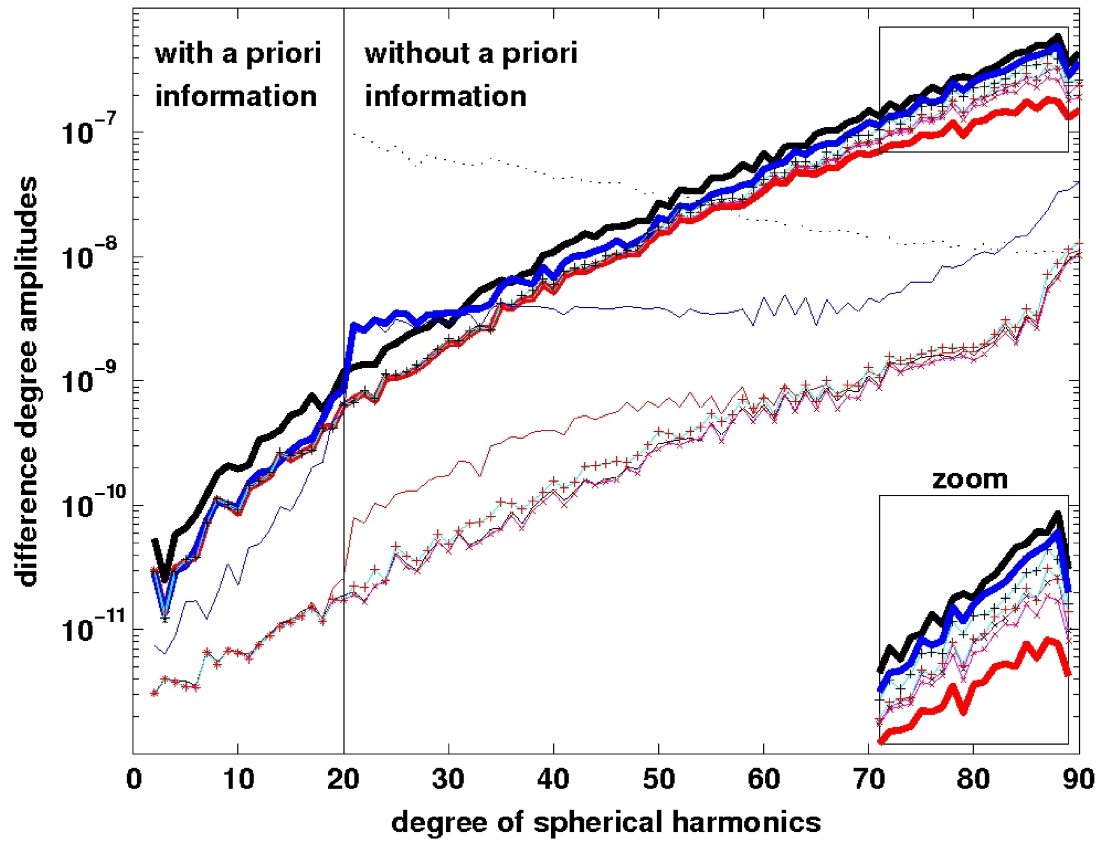

Figure 3: Deviations per degree of the estimated (fully normalized) spherical harmonics w.r.t. the true gravity field coefficients for the solutions **1**, 1x, 1+, **2a**, 2ax, 2a+, **2b**. Observe the only small contribution of **Err.A** to the total effect **Err.N+A** for the majority of the solutions. Deviations above the dashed line (= a priori model for deg.>20, i.e., zero model) indicate no signal content in the corresponding estimates.

30s position sampling:

Solution **2a** performs by the square root of 3 better than solution **1** due to the reduced position noise (see also Fig. 4). The solution is only little affected by **Err.A**: one year of data would have to be accumulated at least in this simulation to decrase the impact of **Err.N** to the same level (see Fig. 5 for data accumulation issues).

Solution **2b** is heavily affected by **Err.A** (see also Fig. 4).

10s position sampling:

Solution 1x (10s kin. positions) provides (theoretically) the best possible GFR resolution. It is affected by **Err.N** at the same level as all other competitive solutions.

Solution 2ax is slightly less affected by **Err.N** (see zoom) than solution 1x and shows virtually no impact of **Err.A**.

"Mean" observation equations:

Solution 2a+ is slightly less affected by **Err.N** (see zoom) than solution 1+ and shows almost no impact of **Err.A**.

Conclusion: All solutions of type **2a** perform (at least slightly) better than the solutions of type **1**. It is thus possible to perform unbiased GFR (30s resolution) with highly reduced-dynamic LEO orbits of type **2a** as the impact of **Err.A** could be almost completely eliminated.

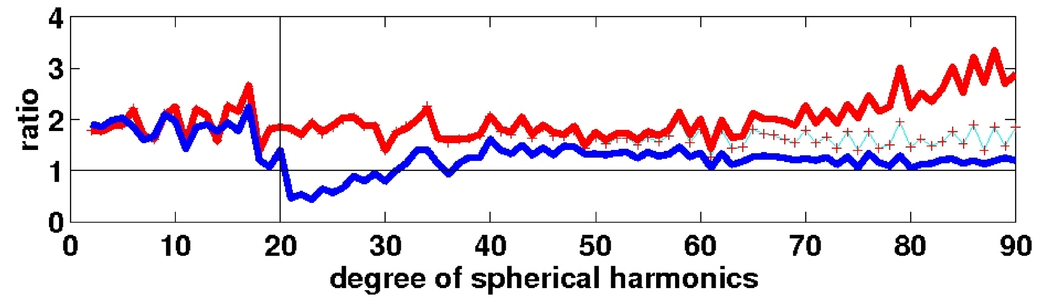

Figure 4: Ratio between the difference degree amplitudes due to **Err.N+A** of solution **1** and solutions **2a**, 2a+, and **2b** (see Table 2 and Fig. 3). Observe that the impact of **Err.N** is reduced by the expected square root of 3 for terms above deg.20 for the solutions **2a** (only little impact of **Err.A**) and 2a+ (almost no impact of **Err.A**), whereas the more pronounced reduction for terms above deg.60 for solution **2a** is a consequence of using only the less noisy positions at the 30s acceleration boundaries. Solution **2b** (heavy impact of **Err.A**) is partially worse than solution **1**, implying that none of the pulse-based solutions of method 2 are suitable for GFR.

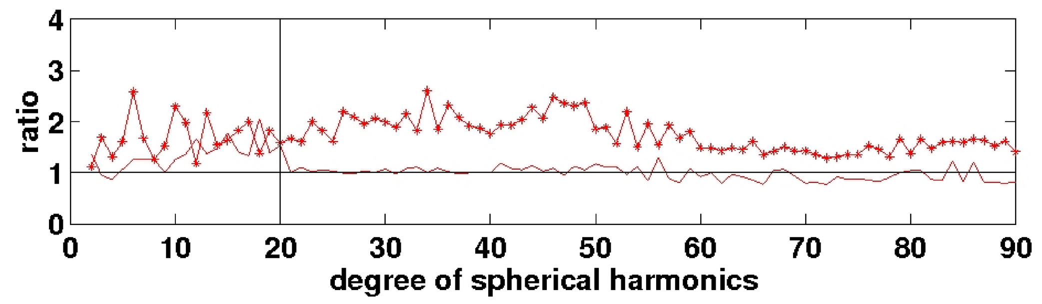

Figure 5: Ratio between the difference degree amplitudes of a 2-day and a 4-day solution of the type **2a** (see Table 2) due to **Err.N** only or due to **Err.A** only. Observe that the impact of **Err.N** is reduced by the expected square root of 2 for terms above deg.60, whereas the more pronounced reduction for degs.20-60 is due to the still inhomogeneous 2-day ground track coverage. Note in particular that the impact of **Err.A** cannot be reduced by the accumulation of data, which becomes relevant in this simulation if (and only if) **Err.N** is reduced to a similar level by accumulation.

Summary and Conclusions

Reduced-dynamic LEO POD methods based on pseudo-stochastic parameters have been compared with the kinematic point positioning method in view of subsequent GFR.

It was shown that reduced-dynamic LEO orbits require at least a spacing of 30s of pseudo-stochastic parameters to be competitive to kinematic orbits for subsequent GFR. Such reduced-dynamic orbits are, however, equivalent to 30s kinematic orbits, if 30s GPS observations are processed, and thus do not offer advantages over the kinematic orbits.

When processing 10s GPS observations, reduced-dynamic LEO orbits based on 30s accelerations are at least equally well (if not slightly better) suited than the kinematic orbits for all probed GFR position sampling techniques in terms of noise. Even the small impact of the deficient a priori gravity field in solution **2a**, which could be overcome in the solutions 2ax or 2a+, would probably not matter in reality as GFR is very likely to be dominated by the presence of much larger systematic effects, e.g., due to a mismodeling of non-gravitational accelerations.

References

Jäggi A, Beutler G, Bock H, Hugentobler U (2005). *Kinematic and highly reduced-dynamic LEO orbit determination for gravity field estimation.* Presented at the Joint Assembly of IAG, IAPSO, and IABO, Cairns, Australia

Jäggi A, Hugentobler U, Beutler G (2006). *Pseudo-stochastic orbit modeling techniques for low-Earth orbiters.* J Geod (in press)

Reigber C, Schwintzer P, Neumayer KH, Barthelmes F, König R, Förste C, Balmino G, Biancale R, Lemoine JM, Loyer S, Bruinsma S, Perosanz F, Fayard T (2003). *The CHAMP-only Earth Gravity Field Model EIGEN-2.* Adv Space Res 31(8): 1883-1888

Svehla D, Rothacher M (2004). *Kinematic precise orbit determination for gravity field determination.* In: Sanso F. (Ed) A window on the future of geodesy. Springer, Berlin Heidelberg New York, pp. 181-188.

UNIVERSITÄT BERN